ORIGINAL PAPER

Nagoya J. Med. Sci. **87**. 509–520, 2025
doi:10.18999/nagjms.87.3.509

Potential effects of microglia-vascular interactions during chronic systemic inflammation in the central nervous system of mice with systemic lupus erythematosus

Mariko Shindo[1], Takahiro Tsuji[1], Rahadian Yudo Hartantyo[1], Yutaro Saito[1,2], Ayaka Ito[3,4,5], Shouta Sugio[1], Ikuko Takeda[1], Takayoshi Suganami[3,4,8] and Hiroaki Wake[1,6,7,8,9]

[1]*Department of Anatomy and Molecular Cell Biology, Nagoya University Graduate School of Medicine, Nagoya, Japan*
[2]*Department of Neurology, Nagoya City University Graduate School of Medical Sciences, Nagoya, Japan*
[3]*Department of Molecular Medicine and Metabolism, Research Institute of Environmental Medicine, Nagoya University, Nagoya, Japan*
[4]*Department of Immunometabolism, Nagoya University Graduate School of Medicine, Nagoya, Japan*
[5]*Institute for Advanced Research, Nagoya University, Nagoya, Japan*
[6]*Division of Multicellular Circuit Dynamics, National Institute for Physiological Sciences, Okazaki, Japan*
[7]*Department of Physiological Sciences, Graduate University for Advanced Studies, SOKENDAI, Hayama, Japan*
[8]*Research Institute for Quantum and Chemical Innovation, Institute of Innovation for Future Society, Nagoya University, Nagoya, Japan*
[9]*Core Research for Evolutional Science and Technology, Japan Science and Technology Agency, Saitama, Japan*

ABSTRACT

Microglia are brain specific macrophages and the only immune cells in the brain. Microglia sense the systemic immune status and contribute to neurological and psychiatric disorders. We previously showed that systemic immune activation induces microglial migration on vessels that regulate the blood brain barrier permeability. In this study, using Toll like receptor 7 induced systemic lupus erythematosus model mice, we found microglia migration on vessels and significant T cell infiltration in the brain. Additionally, microglia interacting with T cell expressed MHC class II molecules in some cases, suggesting the antigen presentation of microglia in systemic lupus erythematosus model mice. This research provides insights on the autoimmune antibody expression in the brain.

Keywords: systemic lupus erythematosus, neurodegenerative diseases, T cell infiltration, microglia, imiquimod

Abbreviations:
BBB: blood-brain barrier
CNS: central nervous system
IMQ: imiquimod
PBS: phosphate-buffered saline
SLE: systemic lupus erythematosus

Received: December 2, 2024; Accepted: January 15, 2025
Corresponding Author: Hiroaki Wake, MD, PhD
Department of Anatomy and Molecular Cell Biology, Nagoya University Graduate School of Medicine, 65 Tsurumai-cho, Showa-ku, Nagoya 466-8550, Japan
Tel: +81-52-744-2000, Fax: +81-52-744-2011, E-mail: wake.hiroaki.r9@f.mail.nagoya-u.ac.jp

INTRODUCTION

Systemic immune status affects neuronal function and performance, ultimately influencing neurological and psychiatric diseases.[1] Acute inflammation causes cognitive dysfunction, whereas chronic inflammation promotes the progression of neurological and psychiatric diseases.[2] Thus the inflammation causes several central nervous system (CNS) pathologies. For instance, maternal inflammation is a risk factor for autism spectrum disorders and schizophrenia, whereas chronic periodontitis is a risk factor for Alzheimer's disease.[3-6] Recent studies have suggested that chronic inflammation promotes cell senescence, cognitive function impairment, and is associated with neurodegenerative diseases.[7]

Microglia are the only immune cells in the CNS and are associated with synaptic functions and the blood-brain barrier (BBB).[8-12] Microglia migrate to vessels with systemic inflammation, which contributes to BBB integrity through microglial claudin-5 expression and their phagocytic functions against astrocyte end-feet.[11] Systemic inflammation increases extracellular adenosine levels and triggers astrocytic activity, which induces a microglial immune response.[13] Several chemokines and cytokines, such as chemokine ligand-2 (CCL2), CCL5, chemokine ligand 1 (CXCL1), and interferon alpha, contribute to the microglial and astrocytic responses.[12,14] These cytokines and chemokines contribute to neurodegenerative disorders by activating the disease-associated microglia (DAM) phenotype.[15,16] In addition, they increase BBB permeability in Alzheimer's disease, Parkinson's disease, multiple sclerosis, depression, schizophrenia, and systemic inflammation, further contributing to the DAM phenotype and disease status.[16,17]

Systemic lupus erythematosus (SLE) is an autoimmune disease that causes systemic inflammation in multiple organs including the lungs, liver, kidneys, and brain. Brain inflammation causes a neuropsychiatric SLE phenotype that triggers psychosis, mood disorders, cognitive dysfunction, and ultimately confusion.[18,19] In some cases,[20-22] patients with neuropsychiatric SLE have autoimmune antibodies such as the anti-N-methyl-D-aspartate receptor, anti-aquaporin-4, and anti-microtubule-associated protein 2. Additionally, BBB permeability increased because of microglial migration via CCL5-chemokine receptor type-5 signaling has been reported.[11] However, whether increased permeability is associated with systemic immune cell invasion is unclear. In this study, we aimed to investigate and elucidate microglia-vascular interactions during chronic systemic inflammation in the CNS of SLE mice induced by a Toll-like receptor 7 agonist (imiquimod, IMQ). IMQ-induced SLE model have been extensively studied using various mouse strains, including FVB/N, BALB/c, and C57BL/6 mice. Topical IMQ treatment in these models has been shown to induce systemic autoimmune features such as splenomegaly, autoantibody production, and immune complex deposition. Additional manifestations include glomerulonephritis, hepatitis, carditis, and photosensitivity, highlighting the utility of this model in mimicking key characteristics of SLE.[23,24] Among these strains, C57BL/6 mice offer significant advantages due to their well-characterized genetic background, which facilitates reproducibility and cross-study comparisons. Previous studies have consistently demonstrated robust and reproducible responses to IMQ treatment in C57BL/6 mice, making them a reliable model for investigating the underlying mechanisms of autoimmune pathogenesis.[23,24] Based on these considerations, we employed C57BL/6 mice in this study in IMQ-induced SLE.

MATERIALS AND METHODS

Animals

Eight-week-old C57BL/6 male mice were used for all experiments to avoid potential variations

during the estrus cycles. The mice had ad libitum access to food and water and with a 12 h light/dark cycle. SLE was induced in mice by a daily topical dose of 50 mg Beselna cream (5% IMQ; Mochida Pharmaceutical Co, Ltd, Tokyo, Japan) on their ears. The mice in the control group received the same dose on both ears, three times a week (Fig. 1A). The Animal Care and Use Committee of Kobe University Graduate School of Medicine, Nagoya University Graduate School of Medicine, and the National Institutes of Natural Sciences approved all experimental protocols. The experiments were conducted in accordance with the National Institutes of Health Guide for the Care and Use of Laboratory Animals.

Complete blood count

Blood samples were collected from the submandibular vein of mice and transferred into tubes (FUJIFILM Wako Pure Chemicals Co, Japan). Complete blood counts were determined using the Celltac Alpha MEK-6550 hematology analyzer (Nihon Kohden, Japan). Plasma was separated by centrifugation at 1200 rpm for 20 minutes. Serum levels of total autoantibodies against double-stranded DNA (dsDNA) were measured using ELISA kits (FUJIFILM Wako Pure Chemicals Co, Japan).

Flow cytometry

The mice were anesthetized with ketamine (74 mg/kg, intraperitoneal injection [i.p.]) and xylazine (10 mg/kg, i.p.) and transcardially perfused with phosphate-buffered saline (PBS). The brains were extracted and immediately immersed in cold Hank's balanced salt solution (HBSS; Gibco-Thermo Fisher Scientific, Waltham, MA, USA). The cerebral cortex, hippocampus, and choroidal plexus were dissected and collected. The tissue samples were dissociated into single cells by incubating them in 0.25% trypsin/EDTA (1 mmol/L) for 30 min at 4 °C, and then incubated for a further 5 min at 37 °C. The trypsin in the homogenate was neutralized with fetal bovine serum (Gibco) and then washed with HBSS containing 0.1 mg/mL DNase (Roche, Basel, Switzerland), followed by centrifugation at 800 × *g* for 5 min. The resulting pellet was resuspended in HBSS and filtered through a 70 μm mesh. Cellular debris was removed by suspending the homogenate in 36% Percoll Plus (Cytiva, Marlborough, MA, USA) and centrifuged at 800 × *g* for 15 min. Residual erythrocytes were lysed using a red blood cell lysis buffer (Roche) for 10 min at 4 °C. The isolated cells were then treated with anti-CD16/32 antibody to block Fc receptors (S17011E; 1:100; BioLegend, San Diego, CA, USA) for 15 min at 4 °C before staining. Antibody staining against CD3ε (FITC conjugated; 145-2C11; 1:100; BioLegend), CD11b (BV711 conjugated; M1/70; 1:100; BioLegend), CD45 (BUV395 conjugated; 30-F11; 1:100; BD Biosciences, Franklin Lakes, NJ, USA), CD4 (APC/Fire 750 conjugated, RM4-4; 1:100; BioLegend), CD8a (BV785 conjugated, 53-6.7; 1:100; BD Biosciences), and Fixable Viability Dye eFluor 506 (1:200; eBioscience, Thermo Fisher Scientific) were conducted for 15 min at 4 °C. Following staining, the samples were processed in PBS containing 1% fetal bovine serum. Stained cells were acquired using Fortessa (BD Biosciences), and data analysis was performed using FACSDiva (BD Biosciences) and FlowJo software (BD Biosciences).

Immunohistochemistry

The mice were anesthetized according to the above. They were then transcardially perfused with a periodate lysine paraformaldehyde (PLP) solution. Fixed brains were extracted from the skull and post-fixed overnight in a PLP solution, followed by submergence in 30% sucrose. The brains were cut into 20 μm slices using a microtome (Leica Microsystems, Wetzlar, Germany). After blocking and permeabilization for 1 h in EzBlock Chemi (ATTO Corporation, Japan) and 0.5% Triton X-100 in PBS, the slices were incubated at 4 °C overnight with primary antibodies

diluted in EzBlock Chemi. After washing with 0.05% Triton X-100 in PBS, the slices were incubated with secondary antibodies in 5% donkey serum, 1% bovine serum albumin, and 0.05% Triton X-100 in PBS at room temperature for 2 h. Thereafter, the slices were mounted on glass slides in fluoromount-G (Southern Biotech Birmingham, AL, USA). The fixed tissue was imaged using a confocal microscope (TiE -A1R; Nikon, Tokyo, Japan) with a ×10 objective (NA 0.45; Nikon) or a ×40 water-immersion objective (NA 1.25; Nikon). The following antibodies were used for staining: anti-IBA1 (1:500; Wako Chemicals, Richmond, VA, USA), anti-TMEM119 (195H4, 1:500; Synaptic Systems, Göttingen, Germany), anti-CD3 (17A2, 1:200; eBioscience), anti-CD3 (1:200; Abcam, Cambridge, United Kingdom), anti-I-A/I-E (M5/114.15.2, 1:200; BioLegend), anti-rabbit Alexa 488, anti-rabbit Alexa 568, anti-mouse Alexa 647, anti-rat Alexa 488, anti-rat Alexa 568 (1:1000 for each; Molecular Probes INC., Eugene, OR, USA). To visualize the brain vasculature and nucleus, brain slices were incubated with DyLight 488-labeled Lycopersicon esculentum LECTIN (1:200; Vector Laboratories, Newark, CA, USA) and hoechst33342 (1:2000; Dojindo Laboratories Co, Ltd, Kumamoto, Japan) at room temperature for 2 h. Imaging was performed using a Nikon TiE-A1 confocal microscope. To detect I-A/I-E-positive IBA1 and CD3+ cells, images of the hippocampus (with each section representing a hemisphere) were captured from five sections from each mouse model. The cortex and hippocampus at 1.45 to 2.88 mm posterior from bregma were analyzed. The imaging resolution was set to 512 pixels, with a step size of 2 μm and a total of five steps. The images were then subjected to z-projection using the SD function in the ImageJ software.[25] Microglia were defined as contact blood vessels (vessel-associated microglia) when the distance along the microglia–blood vessel axis was measured to be below 4 pixels (1 μm), and green fluorescence decreased to zero while the red fluorescence increased from an initial value of zero. The IBA1 positive and CD3+ cells were manually identified via visual inspection.

Behavioral tests

Prior to behavioral testing, the mice were acclimated to the testing environment for 1 h. The tests were performed at least one day apart. After the tests, the equipment was cleaned with sodium hypochlorite solution to eliminate olfactory cues. All tests were performed using DuoMouse.[26]

Elevated plus maze

The elevated plus maze consisted of arms that were 5.5 cm wide and 66.5 cm long. The walls of the closed arms were 20 cm high, and the platform was elevated 50 cm above the floor. The mice were gently placed in the center of the maze and allowed to freely explore for 6 min.

Novelty Y-maze

The mice were allowed to explore the Y-maze, in which one of the three arms was partitioned for 3 min. After the initial exploration, the mice were returned to their cages for 3 min. Subsequently, the partition was removed, and the mice were allowed to explore the Y-maze again for an additional 3 min.

Open field test

The mice were allowed to freely explore a 50 cm × 50 cm open field for 30 min. The middle area was defined as 25% of the field.

Data analysis and statistics

Data were analyzed using GraphPad Prism 10 statistical software (GraphPad Software Inc,

La Jolla, CA, USA). All data are presented as means ± SD values. Statistical significance was assessed using the paired t-test (two-tailed), Unpaired t-test, Mann–Whitney U test (two-tailed), and one-way analysis of variance, followed by Tukey's multiple comparison test and Pearson's correlation analysis. $P < 0.05$ was considered statistically significant.

RESULTS

Phenotypic characterization and behavior analysis

To investigate microglial alterations and infiltration of systemic immune cells in the CNS, pathological properties of the established SLE mouse model were studied (Fig. 1A). The anti-dsDNA antibody levels were significantly higher in IMQ-treated mice than in control vehicle-treated mice (Fig. 1B). Additionally, pancytopenia was observed with a significant reduction in platelet density and hemoglobin levels (Fig. 1C). Furthermore, an enlarged spleen was observed (Fig. 1D).

Elevated plus maze, novelty Y-maze and open field test were used to identify behavioral abnormalities in the mouse model (Fig. 1E–G). The time spent in the open arm of the elevated plus maze was shorter and the central rate in the open field test was decreased in the IMQ-treated mice compared to the control vehicle-treated mice, suggesting anxious behavior (Fig. 1E, G).

T cell infiltration in the CNS

Using flow cytometry (FCM), CD11b–, CD3+, and CD45+ cells were identified, then the CD4/CD8 ratio within these populations were measured (Fig. 2A, B). The ratios of CD3+ and CD45+ cells to total CD11b– cells were significantly higher in the cerebral cortex, hippocampus, and choroid plexus of IMQ-treated mice than in control vehicle-treated mice (Fig. 2C). No significant difference was observed in the CD4+/CD8+ ratio (Fig. 2C). These results suggest that systemic inflammation induces T cell infiltration in the CNS.

Time course of vessel-associated microglia in the CNS

Previous study showed that microglia migrate on vessel to regulate BBB permeability.[11] So we tested whether the microglia in IMQ treated mice also migrate on vessels. Transmembrane protein 119 (Tmem119) is specifically expressed in microglia within the brains of mice and humans.[27] To distinguish microglia from perivascular macrophages, double immunostaining was performed using IBA1 and TMEM119, and cells double-positive for these markers were identified as microglia. The number of microglia in hippocampus associated with vessels was significantly increased in the 6-week IMQ treatment group compared to that in the control group, similar findings were also observed in the 14-week treatment group (Fig. 3A–D).

Antigen presenting microglia in the CNS and their interaction with T cells

To confirm the FCM data, we performed immune-histochemical staining. The density of CD3+ cells was higher in the cerebral cortex, hippocampus, and choroidal plexus, which was consistent with the FCM data (Fig. 4A). Especially in the hippocampus, the number of CD3+ cells interacting with microglia was significantly increased in IMQ-treated mice compared to that of the control vehicle-treated mice (Fig. 4B, C). In addition, the number of microglia expressing MHC class II was higher in IMQ-treated mice than in the control vehicle-treated mice (Fig. 4D, E) and correlated with the number of CD3+ cells infiltrating the CNS (Fig. 4F).

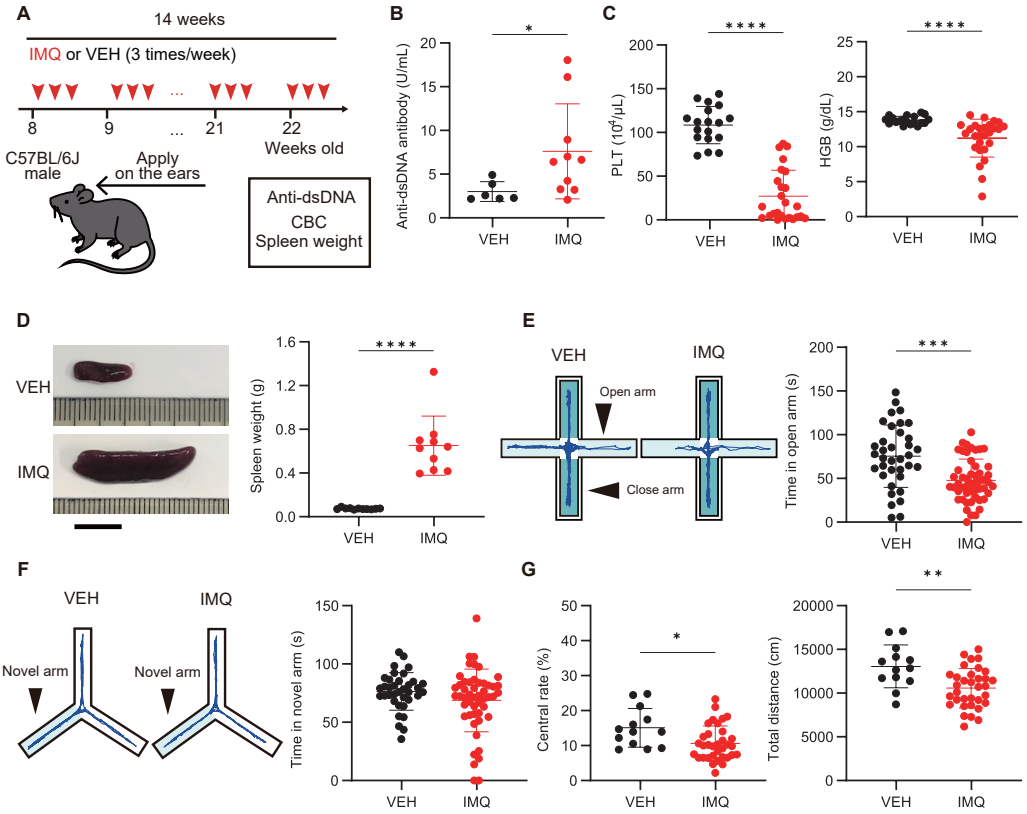

Fig. 1 IMQ-induced SLE model

Fig. 1A: Experimental protocol for IMQ-induced SLE mouse model. Each red triangle represents IMQ or VEH administration.

Fig. 1B: Plasma levels of anti-dsDNA antibodies (VEH, n = 6; IMQ, n = 10).

Fig. 1C: PLT density (VEH, n = 18; IMQ, n = 25) and HGB concentration (VEH, n = 19; IMQ, n = 27).

Fig. 1D: Spleen size and weight in IMQ- and VEH-treated mice (VEH, n = 11; IMQ, n = 10). Scale bar = 10 mm.

Fig. 1E: Typical example of the mouse trajectory in the elevated plus maze. The graph on the right summarizes the time spent in the open arm (VEH, n = 36; IMQ, n = 51).

Fig. 1F: Typical example of the mouse trajectory in the Novelty Y-maze. The graph on the right summarizes the time spent in the novel arm (VEH, n = 36; IMQ, n = 50).

Fig. 1G: Central rate and total distance in open field test (VEH, n = 13; IMQ, n = 34).

Graphs show data from an individual animal overlaid with mean ± SD. *$P < 0.05$, **$P < 0.01$, ***$P < 0.001$, and ****$P < 0.0001$. Unpaired t-test (B, G) or Mann-Whitney U test (C, D, E, F).

SLE: systemic lupus erythematosus
IMQ: imiquimod
VEH: vehicle
dsDNA: double-stranded DNA
PLT: platelet
HGB: hemoglobin

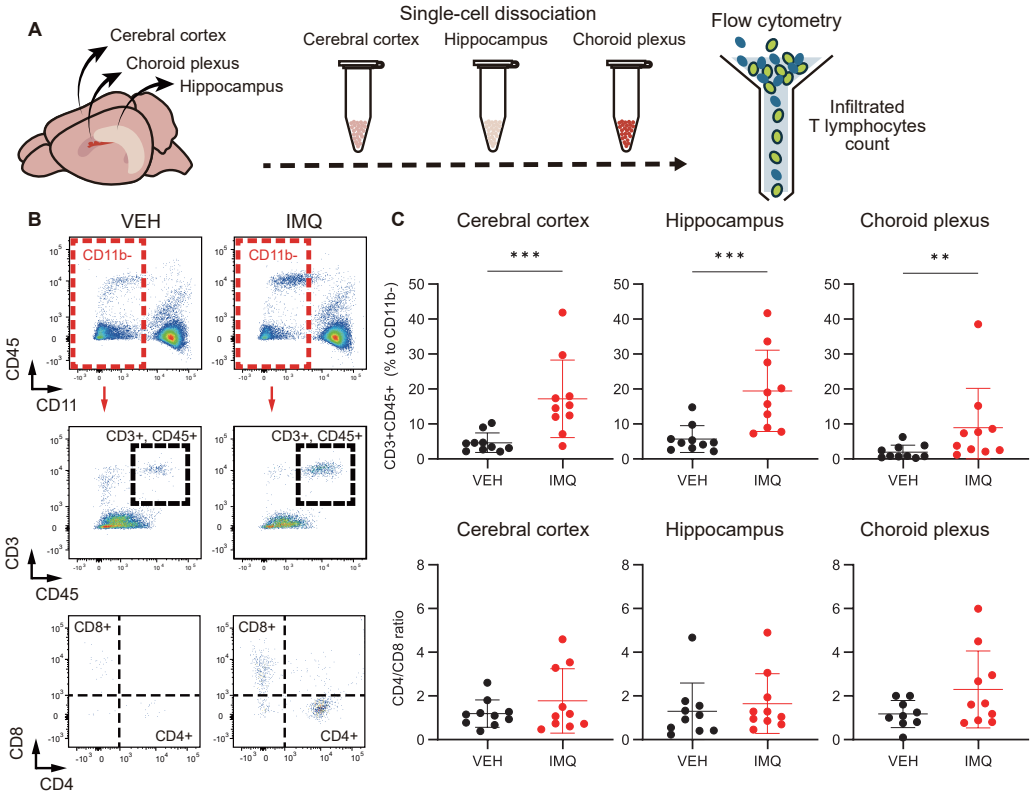

Fig. 2 T lymphocyte infiltration in the CNS of the mouse model

Fig. 2A: Fluorescence-activated cell sorting in the IMQ- and VEH-treated mice. Cells in cerebral cortex, hippocampus, and choroid plexus were dissociated and isolated.

Fig. 2B: FCM assay assessing CD45, CD3, CD8, CD4, and CD11b T cells in IMQ- and VEH-induced SLE mice.

Fig. 2C: CD3+ and CD45+ cell populations to all CD11b− cells in cerebral cortex, hippocampus and choroid plexus (VEH, n = 10; IMQ, n = 10). The CD4/CD8 ratio of CD3+CD45+ cells in cerebral cortex (VEH, n = 10; IMQ, n = 10), hippocampus (VEH, n = 10; IMQ, n = 10) and choroid plexus (VEH, n = 9; IMQ, n = 10).

Graphs show data from an individual animal overlaid with mean ± SD. $^{**}P < 0.01$ and $^{***}P < 0.001$. Mann-Whitney U test.

CNS: central nervous system

IMQ: imiquimod

VEH: vehicle

FCM: flow cytometry

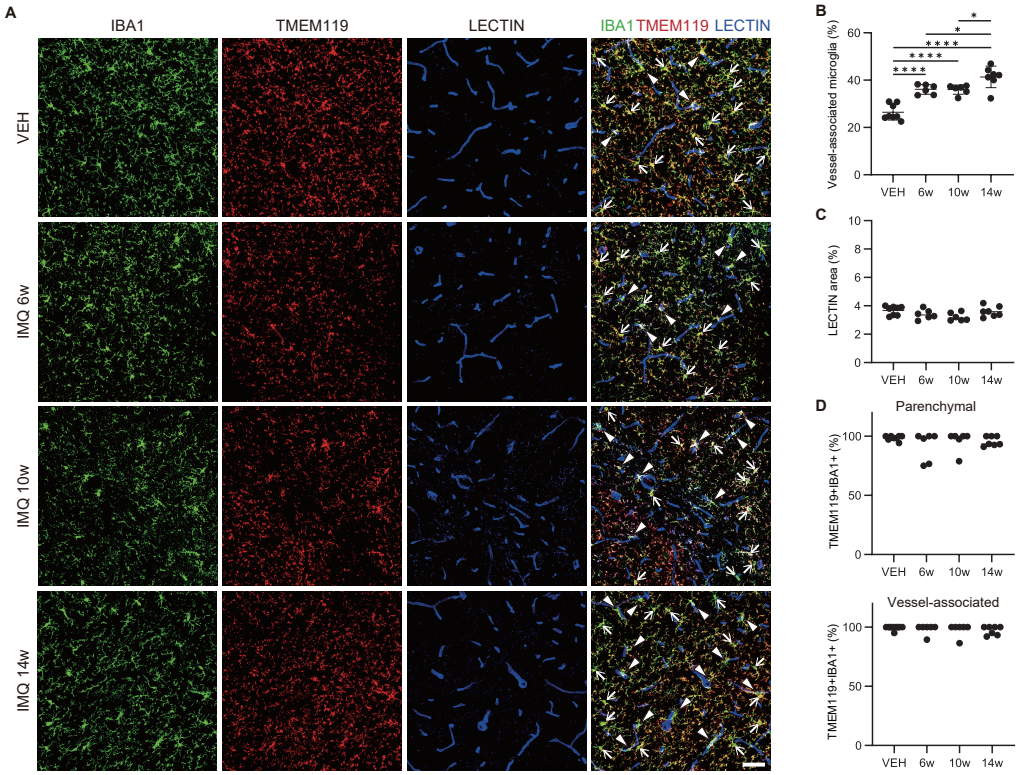

Fig. 3 Density of vessel-associated microglia

Fig. 3A: Images of immunofluorescence demonstrating vessel-associated microglia in hippocampus of mice that were exposed to VEH at 14 weeks or IMQ at 6, 10, and 14 weeks. Arrowheads indicate vessel-associated microglia and arrows indicate parenchymal microglia. IBA1, green; TMEM119, red; LECTIN, blue. Scale bar = 50 μm.

Fig. 3B: The summarized data of the density of vessel-associated microglia.

Fig. 3C: The density of blood vessels in an image field.

Fig. 3D: The proportion of IBA1+ cell expressed TMEM119, respectively.

Graphs show data from an individual animal (VEH, n = 8; IMQ 6 weeks, n = 6; IMQ 10 weeks, n = 6; IMQ 14 weeks, n = 7) overlaid with mean ± SD. *P < 0.05, and **** P < 0.0001. One-way ANOVA followed by Turkey's post hoc test.

IMQ: imiquimod

VEH: vehicle

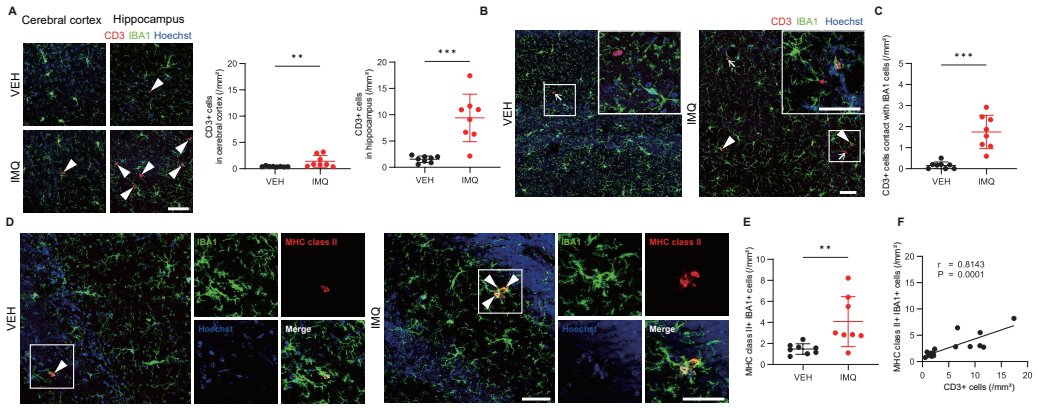

Fig. 4 Distribution of CD3+ cells in CNS of IMQ treated mice

Fig. 4A: CD3+ cells in cerebral cortex and hippocampus of VEH- and IMQ-treated mice, respectively. Arrowheads indicate CD3+ cell. The graph shows the number of CD3+ cells in cerebral cortex and hippocampus, respectively. CD3, red; IBA1, green; Hoechst, blue.

Fig. 4B: Images of CD3+ cells and microglia in hippocampus of VEH- and IMQ-treated mice. Arrowheads indicate CD3+ cells contacted with IBA1+ cells and arrows indicate CD3+ cells not contacted with IBA1+ cells. CD3, red; IBA1, green; Hoechst, blue.

Fig. 4C: The number of CD3+ cells contacted with IBA1+ cells in hippocampus.

Fig. 4D: Images of microglia expressing MHC class II in VEH- and IMQ-treated mice in hippocampus. MHC class II, red; IBA1, green; Hoechst, blue. Arrowheads indicate IBA1+ cells expressing MHC class II.

Fig. 4E: The number of IBA1+ cells expressing MHC class II in hippocampus.

Fig. 4F: The Peason's correlation coefficient between the number of IBA1+ cells expressing MHC class II and CD3+ cells in hippocampus of VEH- and IMQ- treated mice.

Scale bars = 50 μm. Graphs show data from an individual animal (VEH, n = 8; IMQ, n = 8) overlaid with mean ± SD. $^{**}P < 0.01$ and $^{***}P < 0.001$. Mann-Whitney U test.

CNS: central nervous system

IMQ: imiquimod

VEH: vehicle

DISCUSSION

The mice treated with IMQ for 14 weeks showed anti-dsDNA antibodies with decreased hemoglobin and thrombocytopenia; they also presented abnormal behavior. Consistent with previous studies,[23] IMQ-treated C57BL/6 mice exhibited splenomegaly and elevated levels of anti-dsDNA antibodies. In addition, the number of T lymphocytes increased in both the cerebral cortex and hippocampus and was associated with an increased number of T lymphocytes in the choroid plexus, which reflects systemic inflammation. The CNS that invaded T lymphocytes were associated with microglia and microglia expressing MHC class II molecules, suggesting antigen presentation.

Previous murine SLE models have also shown abnormal behavior.[28,29] Moreover, similar murine models, such as the MRL/lupus model exhibits abnormal behavior which is potentially associated with lymphocyte infiltration.[30,31] This suggests that CNS inflammation induced by systemic inflammation causes abnormal behavioral output. Previously, it was determined that microglia migrate to blood vessels during systemic inflammation to regulate the BBB.[11] Systemic inflammation causes endothelial cells to release CCL5, which acts on microglial CCL5-chemokine receptor type-5 to promote its migration to the vessels. These microglia-associated vessels initially protect the BBB via the expression of claudin-5. Prolonged inflammation promotes the

expression of microglial cluster of differentiation-68 and triggers phagocytic activity against astrocyte end-feet to disrupt BBB permeability.[11] In this study, there was an increased number of vessels associated with microglia, which may promote the infiltration of systemic immune cells. In contrast, T cell infiltration was predominantly found in the hippocampus, suggesting that the choroid plexus contributes to the entry route for T cells in the CNS. Previous studies have indicated that T cell infiltrate the CNS via the choroid plexus under pathological conditions.[32,33] This infiltration is promoted by cytokines and chemokines, such as CCL2, CCL3, CCL4, and CXCL10.[34,35] In addition, infiltrated T cell release interleukin (IL)-2, -4, -5, -12, and interferon gamma to induce chronic inflammation for further T cell infiltration and were assumed to exert neuro toxic functions.[36,37] Microglia were found to interact with infiltrating T cells, suggesting that they contribute to antigen presentation.[38] In fact, some patients with SLE accompanied by CNS inflammation show anti-N-methyl-D-aspartate receptor antibodies[39] which have also been suggested to trigger epilepsy in patients with limbic encephalitis.[40] Activated microglia with epileptic seizures release IL-1β, which increases BBB permeability, thereby triggering lymphocyte infiltration.[41,42] Microglia interact with T cells to release cytokines such as IL-1, IL-6, tumor necrosis factor-α, and interferon gamma that promote chronic inflammation in the CNS.[43] More information is required to determine the underlying molecular mechanisms and functional significance of microglia–T cell interactions. Nevertheless, this inhibition could be a therapeutic target for the treatment of CNS lupus.

In conclusion, this study elucidates how brain microglia respond to systemic inflammation and interact with systemic immune cells. Microglia initially migrate to vessels, and prolonged inflammation causes BBB disruption, which promotes T cell infiltration. The infiltrated T cells interacted with microglia and influenced microglial MHC class II expression, suggesting that microglia play an antigen-presenting function in systemic inflammation. This understanding can be used to develop strategies to inhibit chronic inflammation during systemic disease, thereby reducing the susceptibility to cognitive disorders.

AUTHOR CONTRIBUTIONS

M.S.: Investigation, formal analysis. T.T.: Conceptualization, investigation, formal analysis. RY. H., Y.S.: Investigation, data curation. A.I., T.S.: Methodology. S.S., I.T.: Data curation, formal analysis. H.W.: Conceptualization, writing – original draft.

COMPETING INTERESTS

The authors declare no competing interests.

FUNDING

This study was financially supported by the Astellas Foundation for Research on Metabolic Disorders; Grants-in-Aid for Scientific Research on Innovative Areas (19H04753, 19H05219, and 25110732); Grants-in-Aid for Transformative Research Areas (A) (20H05899); Fostering Joint International Research (B) (20KK0170); Grant-in-Aid for Scientific Research (B) (18H02598 and 21H02662). Additionally, it was supported by technical support platforms for promoting research of Advanced Bioimaging Support (JP16H06280), and JST CREST, Grant Numbers JPMJCR1755 and JPMJCR22P6.

ACKNOWLEDGEMENTS

We thank Tsuyako Tatematsu (Nagoya University) for technical assistance and the Uehara Memorial Foundation. We wish to acknowledge Division for Medical Research Engineering, Nagoya University Graduate School of Medicine for usage of Fortessa, FACSDiva and TiE-A1R.

REFERENCES

1 Pluvinage JV, Wyss-Coray T. Systemic factors as mediators of brain homeostasis, ageing and neurodegeneration. *Nat Rev Neurosci*. 2020;21(2):93–102. doi:10.1038/s41583-019-0255-9
2 Zhang W, Xiao D, Mao Q, Xia H. Role of neuroinflammation in neurodegeneration development. *Signal Transduct Target Ther*. 2023;8(1):267. doi:10.1038/s41392-023-01486-5
3 Malkova NV, Yu CZ, Hsiao EY, Moore MJ, Patterson PH. Maternal immune activation yields offspring displaying mouse versions of the three core symptoms of autism. *Brain Behav Immun*. 2012;26(4):607–616. doi:10.1016/j.bbi.2012.01.011
4 Patterson PH. Immune involvement in schizophrenia and autism: etiology, pathology and animal models. *Behav Brain Res*. 2009;204(2):313–321. doi:10.1016/j.bbr.2008.12.016
5 Chen CK, Wu YT, Chang YC. Association between chronic periodontitis and the risk of Alzheimer's disease: a retrospective, population-based, matched-cohort study. *Alzheimers Res Ther*. 2017;9(1):56. doi:10.1186/s13195-017-0282-6
6 Dominy SS, Lynch C, Ermini F, et al. Porphyromonas gingivalis in Alzheimer's disease brains: Evidence for disease causation and treatment with small-molecule inhibitors. *Sci Adv*. 2019;5(1):eaau3333. doi:10.1126/sciadv.aau3333
7 Hu Y, Fryatt GL, Ghorbani M, et al. Replicative senescence dictates the emergence of disease-associated microglia and contributes to Aβ pathology. *Cell Rep*. 2021;35(10):109228. doi:10.1016/j.celrep.2021.109228
8 McNamara NB, Munro DAD, Bestard-Cuche N, et al. Microglia regulate central nervous system myelin growth and integrity. *Nature*. 2023;613(7942):120–129. doi:10.1038/s41586-022-05534-y
9 Wake H, Moorhouse AJ, Jinno S, Kohsaka S, Nabekura J. Resting microglia directly monitor the functional state of synapses in vivo and determine the fate of ischemic terminals. *J Neurosci*. 2009;29(13):3974–3980. doi:10.1523/jneurosci.4363-08.2009
10 Vasek MJ, Garber C, Dorsey D, et al. A complement-microglial axis drives synapse loss during virus-induced memory impairment. *Nature*. 2016;534(7608):538–543. doi:10.1038/nature18283
11 Haruwaka K, Ikegami A, Tachibana Y, et al. Dual microglia effects on blood brain barrier permeability induced by systemic inflammation. *Nat Commun*. 2019;10(1):5816. doi:10.1038/s41467-019-13812-z
12 Kirkley KS, Popichak KA, Afzali MF, Legare ME, Tjalkens RB. Microglia amplify inflammatory activation of astrocytes in manganese neurotoxicity. *J Neuroinflammation*. 2017;14(1):99. doi:10.1186/s12974-017-0871-0
13 Guo Q, Gobbo D, Zhao N, et al. Adenosine triggers early astrocyte reactivity that provokes microglial responses and drives the pathogenesis of sepsis-associated encephalopathy in mice. *Nat Commun*. 2024;15(1):6340. doi:10.1038/s41467-024-50466-y
14 Bose S, Cho J. Role of chemokine CCL2 and its receptor CCR2 in neurodegenerative diseases. *Arch Pharm Res*. 2013;36(9):1039–1050. doi:10.1007/s12272-013-0161-z
15 Keren-Shaul H, Spinrad A, Weiner A, et al. A Unique Microglia Type Associated with Restricting Development of Alzheimer's Disease. *Cell*. 2017;169(7):1276–1290.e17. doi:10.1016/j.cell.2017.05.018
16 Baik SH, Kang S, Lee W, et al. A Breakdown in Metabolic Reprogramming Causes Microglia Dysfunction in Alzheimer's Disease. *Cell Metab*. 2019;30(3):493–507.e6. doi:10.1016/j.cmet.2019.06.005
17 Butovsky O, Jedrychowski MP, Moore CS, et al. Identification of a unique TGF-β-dependent molecular and functional signature in microglia. *Nat Neurosci*. 2014;17(1):131–143. doi:10.1038/nn.3599
18 Hanly JG, Urowitz MB, Su L, et al. Prospective analysis of neuropsychiatric events in an international disease inception cohort of patients with systemic lupus erythematosus. *Ann Rheum Dis*. 2010;69(3):529–535. doi:10.1136/ard.2008.106351
19 Schwartz N, Stock AD, Putterman C. Neuropsychiatric lupus: new mechanistic insights and future treatment directions. *Nat Rev Rheumatol*. 2019;15(3):137–152. doi:10.1038/s41584-018-0156-8
20 Lu XY, Chen XX, Huang LD, Zhu CQ, Gu YY, Ye S. Anti-alpha-internexin autoantibody from neuropsychiatric lupus induce cognitive damage via inhibiting axonal elongation and promote neuron apoptosis. *PLoS One*. 2010;5(6):e11124. doi:10.1371/journal.pone.0011124

21 Závada J, Nytrová P, Wandinger KP, et al. Seroprevalence and specificity of NMO-IgG (anti-aquaporin 4 antibodies) in patients with neuropsychiatric systemic lupus erythematosus. *Rheumatol Int*. 2013;33(1):259–263. doi:10.1007/s00296-011-2176-4

22 Williams RC Jr, Sugiura K, Tan EM. Antibodies to microtubule-associated protein 2 in patients with neuropsychiatric systemic lupus erythematosus. *Arthritis Rheum*. 2004;50(4):1239–1247. doi:10.1002/art.20156

23 Yokogawa M, Takaishi M, Nakajima K, et al. Epicutaneous application of toll-like receptor 7 agonists leads to systemic autoimmunity in wild-type mice: a new model of systemic Lupus erythematosus. *Arthritis Rheumatol*. 2014;66(3):694–706. doi:10.1002/art.38298

24 Nomura A, Mizuno M, Noto D, et al. Different Spatial and Temporal Roles of Monocytes and Monocyte-Derived Cells in the Pathogenesis of an Imiquimod Induced Lupus Model. *Front Immunol*. 2022;13:764557. doi:10.3389/fimmu.2022.764557

25 Schindelin J, Arganda-Carreras I, Frise E, et al. Fiji: an open-source platform for biological-image analysis. *Nat Methods*. 2012;9(7):676–682. doi:10.1038/nmeth.2019

26 Arakawa T, Tanave A, Ikeuchi S, et al. A male-specific QTL for social interaction behavior in mice mapped with automated pattern detection by a hidden Markov model incorporated into newly developed freeware. *J Neurosci Methods*. 2014;234:127–134. doi:10.1016/j.jneumeth.2014.04.012

27 Bennett ML, Bennett FC, Liddelow SA, et al. New tools for studying microglia in the mouse and human CNS. *Proc Natl Acad Sci U S A*. 2016;113(12):E1738–E1746. doi:10.1073/pnas.1525528113

28 Sakić B, Szechtman H, Keffer M, Talangbayan H, Stead R, Denburg JA. A behavioral profile of autoimmune lupus-prone MRL mice. *Brain Behav Immun*. 1992;6(3):265–285. doi:10.1016/0889-1591(92)90048-s

29 Sakić B, Szechtman H, Denburg S, Carbotte R, Denburg JA. Spatial learning during the course of autoimmune disease in MRL mice. *Behav Brain Res*. 1993;54(1):57–66. doi:10.1016/0166-4328(93)90048-u

30 Stock AD, Wen J, Doerner J, Herlitz LC, Gulinello M, Putterman C. Neuropsychiatric systemic lupus erythematosus persists despite attenuation of systemic disease in MRL/lpr mice. *J Neuroinflammation*. 2015;12:205. doi:10.1186/s12974-015-0423-4

31 Sakić B, Szechtman H, Stead RH, Denburg JA. Joint pathology and behavioral performance in autoimmune MRL-lpr Mice. *Physiol Behav*. 1996;60(3):901–905. doi:10.1016/0031-9384(96)00065-0

32 Moore E, Huang MW, Reynolds CA, Macian F, Putterman C. Choroid Plexus-Infiltrating T Cells as Drivers of Murine Neuropsychiatric Lupus. *Arthritis Rheumatol*. 2022;74(11):1796–1807. doi:10.1002/art.42252

33 Moore E, Bharrhan S, Rao DA, Macian F, Putterman C. Characterisation of choroid plexus-infiltrating T cells reveals novel therapeutic targets in murine neuropsychiatric lupus. *Ann Rheum Dis*. 2024;83(8):1006–1017. doi:10.1136/ard-2023-224689

34 Babcock AA, Kuziel WA, Rivest S, Owens T. Chemokine expression by glial cells directs leukocytes to sites of axonal injury in the CNS. *J Neurosci*. 2003;23(21):7922–7930. doi:10.1523/jneurosci.23-21-07922.2003

35 Laurent C, Dorothée G, Hunot S, et al. Hippocampal T cell infiltration promotes neuroinflammation and cognitive decline in a mouse model of tauopathy. *Brain*. 2017;140(1):184–200. doi:10.1093/brain/aww270

36 Brochard V, Combadière B, Prigent A, et al. Infiltration of CD4+ lymphocytes into the brain contributes to neurodegeneration in a mouse model of Parkinson disease. *J Clin Invest*. 2009;119(1):182–192. doi:10.1172/jci36470

37 Jin R, Yang G, Li G. Inflammatory mechanisms in ischemic stroke: role of inflammatory cells. *J Leukoc Biol*. 2010;87(5):779–789. doi:10.1189/jlb.1109766

38 Chen X, Firulyova M, Manis M, et al. Microglia-mediated T cell infiltration drives neurodegeneration in tauopathy. *Nature*. 2023;615(7953):668–677. doi:10.1038/s41586-023-05788-0

39 Lapter S, Marom A, Meshorer A, et al. Amelioration of brain pathology and behavioral dysfunction in mice with lupus following treatment with a tolerogenic peptide. *Arthritis Rheum*. 2009;60(12):3744–3754. doi:10.1002/art.25013

40 Graus F, Titulaer MJ, Balu R, et al. A clinical approach to diagnosis of autoimmune encephalitis. *Lancet Neurol*. 2016;15(4):391–404. doi:10.1016/s1474-4422(15)00401-9

41 Rüber T, David B, Lüchters G, et al. Evidence for peri-ictal blood-brain barrier dysfunction in patients with epilepsy. *Brain*. 2018;141(10):2952–2965. doi:10.1093/brain/awy242

42 Ravizza T, Gagliardi B, Noé F, Boer K, Aronica E, Vezzani A. Innate and adaptive immunity during epileptogenesis and spontaneous seizures: evidence from experimental models and human temporal lobe epilepsy. *Neurobiol Dis*. 2008;29(1):142–160. doi:10.1016/j.nbd.2007.08.012

43 Smith JA, Das A, Ray SK, Banik NL. Role of pro-inflammatory cytokines released from microglia in neurodegenerative diseases. *Brain Res Bull*. 2012;87(1):10–20. doi:10.1016/j.brainresbull.2011.10.004